

See discussions, stats, and author profiles for this publication at: <https://www.researchgate.net/publication/231273714>

# Measurement of the Liquid–Deposit Interface Temperature during Solids Deposition from Wax–Solvent Mixtures under Sheared Cooling

ARTICLE *in* ENERGY & FUELS · SEPTEMBER 2008

Impact Factor: 2.79 · DOI: 10.1021/ef800542a

---

CITATIONS

13

---

READS

40

2 AUTHORS, INCLUDING:



Anil K Mehrotra

The University of Calgary

160 PUBLICATIONS 2,348 CITATIONS

SEE PROFILE

## Article

### Measurement of the Liquid#Deposit Interface Temperature during Solids Deposition from Wax#Solvent Mixtures under Sheared Cooling

Hamid Bidmus, and Anil K. Mehrotra

*Energy Fuels*, **2008**, 22 (6), 4039-4048 • Publication Date (Web): 01 October 2008

Downloaded from <http://pubs.acs.org> on November 21, 2008

## More About This Article

Additional resources and features associated with this article are available within the HTML version:

- Supporting Information
- Access to high resolution figures
- Links to articles and content related to this article
- Copyright permission to reproduce figures and/or text from this article

[View the Full Text HTML](#)



**ACS Publications**  
High quality. High impact.

Energy & Fuels is published by the American Chemical Society, 1155 Sixteenth Street N.W., Washington, DC 20036

# Measurement of the Liquid–Deposit Interface Temperature during Solids Deposition from Wax–Solvent Mixtures under Sheared Cooling

Hamid Bidmus and Anil K. Mehrotra\*

Department of Chemical and Petroleum Engineering, University of Calgary, Calgary, Alberta, Canada T2N 1N4

Received July 8, 2008. Revised Manuscript Received August 7, 2008

The liquid-deposit interface temperature for solids deposition was measured under sheared as well as static cooling from prepared mixtures of two petroleum waxes and a multicomponent paraffinic solvent ( $C_9$ – $C_{16}$ ) at different coolant temperatures. The interface temperature and location were obtained from the rate of change of temperature at fixed radial locations in a cylindrical vessel, while maintaining the coolant temperature below the wax appearance temperature (WAT) of the wax–solvent mixture. In addition, precipitation-filtration experiments were performed on several wax–solvent mixtures at a temperature below the respective WAT, which confirmed that the WAT of the filtrate was 1–2 °C less than the precipitation and filtration temperature. For all sheared- and static-cooling experiments, with both wax samples, the interface temperature throughout the deposit-growth process was found to be equal to the WAT of the liquid phase. The results of this study validate the constant-interface-temperature assumption made in the heat-transfer approach for modeling solids deposition from waxy mixtures but do not support the increasing-interface-temperature assumption in the molecular-diffusion approach.

## Introduction

The exposure of a “waxy” petroleum crude oil to cooler temperatures is known to cause the precipitation, crystallization, and deposition of heavier hydrocarbons on cold surfaces. The deposition of waxy solids results in high pressure drops and increased energy consumption during crude oil transportation. In petroleum production and processing, solids deposition causes a decrease in process flow rates, thereby affecting the efficiency of the operations.

Upon cooling of “waxy” crude oils, the temperature at which the first wax particles are formed is known as the wax appearance temperature (WAT). The WAT of prepared wax–solvent mixtures has been shown to be lower than the wax disappearance temperature (WDT, measured during heating), which was found to be closer to the thermodynamic liquidus temperature.<sup>1</sup> The crystallization of heavier hydrocarbons (carbon numbers greater than about 18–20), is caused by their decreased solubility at temperatures below the WAT, which can lead to deposition with as little as 2% of precipitated wax solids.<sup>2,3</sup> The deposit layer thus formed is comprised of both liquid and solid phases in a gel-like structure.<sup>4</sup> Visual observations of deposits have shown the solid and liquid phases to be

platelet-shaped wax crystallites that overlap and interlock around the liquid crude oil.<sup>4</sup>

Some of the important factors that are relevant for the deposit formation include wax concentration, oil temperature and flow rate, and pipe-wall temperature. Previous studies have shown that the mass of deposited wax decreases as the flow rate is increased under laminar flow,<sup>3,5–12</sup> and the same trend was also observed for deposition under turbulent flow.<sup>13</sup> An increase in the flow rate causes an increase in the deposit wax content.<sup>3,8,11–13</sup> The shear history of the crude oil is also an important factor.<sup>14</sup>

Different mechanisms and modeling approaches for the deposition process have been proposed.<sup>15,16</sup> One of the com-

\* Corresponding author. Phone: (403) 220-7406. Fax: (403) 284-4852. E-mail: mehrotra@ucalgary.ca.

(1) Bhat, N. V.; Mehrotra, A. K. Measurement and Prediction of Phase Behavior of Wax-solvent Mixtures: Significance of the Wax Disappearance Temperature. *Ind. Eng. Chem. Res.* **2004**, *43*, 3451.

(2) Holder, G. A.; Winkler, J. Wax Crystallization from Distillate Fuels. II. Mechanism of Pour Depression. *J. Inst. Pet.* **1965**, *51*, 235.

(3) Singh, P.; Venkatesan, R.; Fogler, H. S.; Nagarajan, N. Formation and Aging of Incipient Thin Film Wax-Oil Gels. *AIChE J.* **2000**, *46*, 1059.

(4) Holder, G. A.; Winkler, J. Wax Crystallization from Distillate Fuels. I. Cloud and Pour Phenomena Exhibited by Solutions of Binary n-Paraffin Mixtures. *J. Inst. Pet.* **1965**, *51*, 228.

(5) Patton, C. C.; Casad, B. M. Paraffin Deposition from Refined Wax-solvent Systems. *Soc. Pet. Eng. J.* **1970**, *10* (1), 17.

(6) Bott, T. R.; Gudmunsson, J. S. Deposition of Paraffin Wax from Kerosene in Cooled Heat Exchanger Tubes. *Can. J. Chem. Eng.* **1977**, *55*, 381.

(7) Creek, J. L.; Lund, H. J.; Brill, J. P.; Volk, M. Wax Deposition in Single Phase Flow. *Fluid Phase Equilib.* **1999**, *801*, 158.

(8) Singh, P.; Venkatesan, R.; Fogler, H. S.; Nagarajan, N. Morphological Evolution of Thick Wax Deposits during Aging. *AIChE J.* **2001**, *47*, 6.

(9) Wu, C.; Wang, K. S.; Shuler, P. J.; Tand, Y.; Creek, J. L.; Carlson, R. M.; Cheung, S. Measurement of Wax Deposition in Paraffin Solutions. *AIChE J.* **2002**, *48*, 2107.

(10) Jennings, D. W.; Weispfennig, K. Effects of Shear and Temperature on Wax Deposition: Coldfinger Investigation with a Gulf of Mexico Crude Oil. *Energy Fuels* **2005**, *19*, 1376.

(11) Bidmus, H. O.; Mehrotra, A. K. Heat-Transfer Analogy for Wax Deposition from Paraffinic Mixtures. *Ind. Eng. Chem. Res.* **2004**, *43*, 791.

(12) Parthasarathi, P.; Mehrotra, A. K. Solids Deposition from Multicomponent Wax-solvent Mixtures in a Benchscale Flow-Loop Apparatus with Heat Transfer. *Energy Fuels* **2005**, *19*, 1387.

(13) Fong, N.; Mehrotra, A. K. Deposition under Turbulent Flow of Wax-Solvent Mixtures in a Bench-Scale Flow-Loop Apparatus with Heat Transfer. *Energy Fuels* **2007**, *21*, 1263.

(14) Cawkwell, M. G.; Charles, M. E. Start-up of Pipelines containing Gelled Crude Oils: Comparison of Improved Model and Pilot Pipeline Data. *J. Pipelines* **1989**, *7* (3), 265.

monly accepted modeling approaches for wax deposition is molecular diffusion. This modeling approach is based on the premise that the amount of deposited solids can be estimated through the radial transport of wax molecules that is caused by a radial concentration gradient. This concentration gradient is induced by the temperature gradient resulting from the difference between the flowing bulk crude oil temperature (higher than the WAT) and the liquid–deposit interface temperature (assumed to be lower than the WAT). In the molecular-diffusion approach, the temperature at the interface is assumed to vary, increasing gradually from an initial value, close to the pipe-wall temperature, to the WAT at steady state. Singh et al.<sup>3</sup> presented a plot of predicted changes in the liquid–deposit interface temperature with time that were back-calculated from an energy balance; however, these predictions were not validated with any experimental measurements. The molecular-diffusion approach relies on the increasing-interface-temperature assumption because the concentration driving force would exist only if the interface temperature during deposit formation is below the WAT.

Recent studies have proposed a different approach, based on heat transfer, for solids deposition from waxy mixtures.<sup>11–13,17–22</sup> In the heat-transfer modeling approach, the solids deposition process is treated to be essentially (partial) freezing or solidification.<sup>18–21</sup> The rate of heat transfer through the deposit layer is dependent on the thermal driving force between the bulk crude oil temperature and the cooler pipe-wall temperature. It is also influenced by the latent heat released during the phase transformation of the crude oil or wax–solvent mixture into solid at the interface and within the deposit-layer and by convective and/or conductive thermal resistances in series. The main assumption in the heat-transfer approach is that the liquid–deposit interface temperature,  $T_d$ , remains constant and equal to the WAT of the crude oil or wax–solvent mixture throughout the deposition process.

Recent laboratory investigations<sup>11–13</sup> reported a relatively rapid attainment (within 0.5–1 h) of thermal pseudosteady-state during wax deposition from paraffinic mixtures under laminar as well as turbulent flow conditions. Results from these experimental studies confirmed that  $T_d$  is equal to the WAT of the wax–solvent mixture at thermal pseudosteady-state for both laminar and turbulent flows.<sup>11–13</sup> The predicted deposit mass from the steady-state heat-transfer model correlated well with the data. It was also identified that the temperature difference across the deposit layer is an important parameter in the deposition process. A dimensionless parameter, defined as the ratio of the temperature difference across the deposit layer to

the overall temperature difference, was shown to be related to the mass of deposited solids.<sup>11–13</sup>

The heat-transfer-based model, incorporating the moving boundary problem formulation, is based on the assumption that  $T_d$  is equal to WAT throughout the deposition process.<sup>18–21</sup> This is different from the molecular-diffusion approach, in which, as previously mentioned, the key assumption is that  $T_d$  varies during deposit-growth, starting from an initial value close to the pipe-wall temperature and increasing gradually to reach the WAT at steady-state.<sup>3,8,22–24</sup> Thus, the two modeling approaches differ in their treatment of the liquid–deposit interface temperature,  $T_d$ , during the transient deposition stage. A direct measurement of  $T_d$  during the transient deposition process, under flowing conditions in a pipeline, is a challenging task because the interface location would continue to move radially with time even at the same axial location. It would be difficult to insert an instrument for temperature measurement into the pipeline with flowing crude oil without affecting the deposit being formed. Likewise, it would be difficult to carry out an *in situ* analysis of the deposit-layer because, as mentioned above, it consists of liquid and solid phases, whose ratio and properties are sensitive to changes in temperature and hydrodynamic conditions.

In an attempt to resolve the underlying uncertainty concerning  $T_d$ , a recent study reported experimental results for the interface temperature during the cooling of prepared wax–solvent mixtures under static conditions.<sup>25</sup> The static cooling of the wax–solvent mixtures was carried out in a cylindrical vessel using two different surface areas with thermocouples placed at fixed radial locations for monitoring the temperatures. The results indicated that the interface temperature, during the deposit-layer growth under static cooling, remained constant at the WAT of the liquid phase.<sup>25</sup> It provided validation of the constant-interface-temperature assumption made in the heat-transfer approach for modeling the deposition of solids from waxy mixtures. However, the interface temperature was measured only under static conditions, that is, without any induced shear. Furthermore, experimental evidence was not provided to validate the assumption that the interface temperature, when the wax–solvent mixture temperature fell below its WAT (giving rise to wax crystals suspended in the liquid phase), was equal to the WAT of the resultant liquid phase.

This study reports additional results as a follow-up on those previously reported from the static deposition experiments<sup>25</sup> and involve the effects of two additional variables. First, the interface temperature measurements, under static cooling conditions, are reported with another multicomponent wax sample with significantly different properties. Second, the interface temperature measurements under two levels of induced shear stress are reported. In addition, precipitation and filtration experiments with wax–solvent mixtures were performed for validating the assumption that the interface temperature below the WAT (leading to wax crystals suspended in the liquid phase) is equal to the WAT of the liquid phase. These precipitation-filtration tests involved cooling several wax–solvent mixtures to a temperature below their WAT, the separation of precipitated

(15) Burger, E. D.; Perkins, T. K.; Striegler, J. H. Studies of Wax Deposition in the Trans Alaska Pipeline. *J. Petrol. Technol.* **1981**, 33, 1075.

(16) Azevedo, L. F. A.; Teixeira, A. M. A Critical Review of the Modeling of Wax Deposition Mechanisms. *Petrol. Sci. Technol.* **2003**, 21, 393.

(17) Cordoba, A. J.; Schall, C. A. Application of a Heat Transfer Method to determine Wax Deposition in a Hydrocarbon Binary Mixture. *Fuel* **2001**, 80, 1285.

(18) Merino-Garcia, D.; Margarone, M.; Corra, S. Kinetics of Waxy Gel Formation from Batch Experiments. *Energy Fuels* **2007**, 21, 1287.

(19) Mehrotra, A. K.; Bhat, N. V. Modeling the Effect of Shear Stress on Deposition from “Waxy” Mixtures under Laminar Flow with Heat Transfer. *Energy Fuels* **2007**, 21, 1277.

(20) Bhat, N. V.; Mehrotra, A. K. Modeling of Deposit Formation from “Waxy” Mixtures via Moving Boundary Formulation: Radial Heat Transfer under Static and Laminar Flow Conditions. *Ind. Eng. Chem. Res.* **2005**, 44, 6948.

(21) Bhat, N. V.; Mehrotra, A. K. Modeling of Deposition from “Waxy” Mixtures in a Pipeline under Laminar Flow Conditions via Moving Boundary Formulation. *Ind. Eng. Chem. Res.* **2006**, 45, 8728.

(22) Svendsen, J. A. Mathematical Modeling of Wax Deposition in Oil Pipeline Systems. *AIChE J.* **1993**, 39, 1377.

(23) Kok, M. V.; Saracoglu, R. O. Mathematical Modeling of Wax Deposition in Crude Oil Pipelines (Comparative Study). *Pet. Sci. Tech.* **2000**, 18, 1121.

(24) Ramirez-Jaramillo, E.; Lira-Galeana, C.; Manero, O. Modeling Wax Deposition in Pipelines. *Pet. Sci. Tech.* **2004**, 22, 821.

(25) Bidmus, H. O.; Mehrotra, A. K. Measurement of the Liquid-deposit Interface Temperature during Solids Deposition from Wax-solvent Mixtures under Static Cooling Conditions. *Energy Fuels* **2008**, 22, 1174.

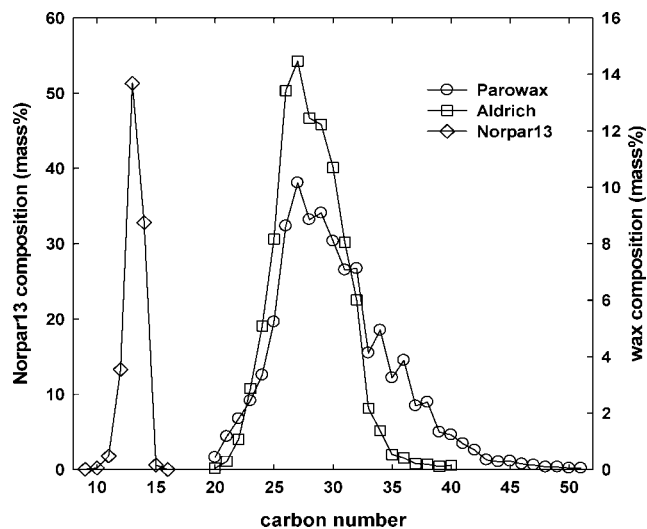


Figure 1. Carbon number distributions of Aldrich and Parowax samples and Norpar13.<sup>1,11–13,25</sup>

solids from the liquid (filtrate) phase by filtration, and the measurement of the WAT and WDT of the filtrate.

### Experimental Section

**Materials.** All experiments were carried out with prepared mixtures of paraffinic waxes in a petroleum solvent. The wax sample used in the previous study,<sup>25</sup> called “Aldrich” and obtained from Sigma-Aldrich (Ontario, Canada), was used in sheared-cooling experiments. Another wax sample, called “Parowax” and obtained from Conros Corp (Ontario, Canada), was used in static-cooling experiments. Simulated distillation (GC) analysis showed that the Aldrich wax consisted of *n*-alkanes ranging from C<sub>20</sub> to C<sub>40</sub>,<sup>1,11,12,25,26</sup> whereas the Parowax sample consisted of *n*-alkanes over the range of C<sub>20</sub> to C<sub>50</sub>.<sup>13</sup> Figure 1 shows the carbon number distribution of both waxes. The Aldrich wax, with a narrower carbon number distribution than the Parowax sample, had higher concentrations of C<sub>24</sub>–C<sub>31</sub>. The Parowax sample, on the other hand, showed a wider carbon number distribution with higher concentrations of constituents with carbon number greater than C<sub>31</sub>. The average molar mass of the Parowax sample was calculated to be 414.2 kg kmol<sup>−1</sup>, which is equivalent to a mean carbon number of about 29. The Aldrich wax had an average molar mass of 390.8 kg kmol<sup>−1</sup>, which corresponds to a mean carbon number of about 28.

Norpar13, obtained from Imperial Oil (Ontario, Canada), was used as the solvent for preparing all wax–solvent mixtures. The carbon number distribution of Norpar13 is also plotted in Figure 1. Norpar13 consisted of *n*-alkanes ranging from C<sub>9</sub> to C<sub>16</sub>, with a density of 754 kg m<sup>−3</sup> at 23 °C.<sup>1,12,13</sup> The average molar mass of Norpar13 was calculated to be 185.7 kg kmol<sup>−1</sup>, which corresponds to an average carbon number of about 13.

**WAT and PPT Measurements.** Wax–solvent mixtures were prepared with the two waxes, Parowax and Aldrich, and used in the experiments carried out in this study. The WAT and pour point temperature (PPT) of these mixtures were measured using a visual method with cooling steps of 1 °C.<sup>1,11–13,25,26</sup> The mixtures were cooled at a rate of 0.25 °C min<sup>−1</sup> and maintained isothermally at each 1 °C cooling step for 30 min. Hence, the uncertainty associated with the WAT and PPT measurements is up to +1 °C, indicating that the actual WAT (or PPT) could be between the measured WAT and WAT + 1 °C (or the measured PPT and PPT + 1 °C). Table 1 and Figure 2 show the measured WAT and PPT values for the different compositions of wax–solvent mixtures. Results for Aldrich–Norpar13 mixtures are for 8, 9, and 20 mass % wax,

Table 1. WAT and PPT Values for Wax–Norpar13 Mixtures

Aldrich–Norpar13			Parowax–Norpar13		
wax concentration	WAT	PPT	wax concentration	WAT	PPT
(mass %)	(°C)	(°C)	(mass %)	(°C)	(°C)
8	26	22	2	28	<2
9	27	23	3	30	8
20	34	31	4	32	17
			5	34	20
			6	35	24
			20	43	37

whereas those for Parowax–Norpar13 mixtures are for 2–6 mass % and 20 mass % wax. These results show that both WAT and PPT of Parowax–Norpar13 mixtures are higher than those of Aldrich–Norpar13 mixtures. As a comparison, the 20 mass % Aldrich–Norpar13 mixture and the 5 mass % Parowax–Norpar13 mixture have the same WAT of 34 ± 1 °C.

**Precipitation-Filtration Tests.** When a wax–solvent mixture is slowly cooled to a temperature below its WAT (but higher than its PPT), wax crystals are formed and remain suspended in the liquid phase. Each precipitation–filtration experiment involved the cooling of a prepared wax–solvent mixture of known composition at a constant rate of 0.25 °C min<sup>−1</sup> to the laboratory temperature (which was below its WAT), which caused the precipitation of wax crystals. After holding it isothermally, the wax–solvent mixture separated into solid and liquid phases. The two-phase mixture was then filtered under vacuum using a 2.5 μm filter paper, and the filtrate was observed to be clear (without any noticeable solid particles). The WAT and WDT of the filtrate were measured using the visual method described before. Note that all precipitation–filtration tests were performed at laboratory temperature (about 25 °C), which was between the WAT and PPT of all wax–solvent mixtures given in Table 1 (except 20 mass % mixtures, which were not used in the precipitation–filtration tests). The average laboratory temperature for the precipitation–filtration tests with Parowax mixtures was 25.3 °C, but it was 24.6 °C for the tests with Aldrich mixtures; hence, the Parowax and Aldrich mixtures were cooled, before filtering, to 26 and 25 °C, respectively.

The results obtained from these tests are given in Table 2. The WAT of all the filtrates was found to be about 1 °C less than the average laboratory or precipitation–filtration temperature. All Parowax–Norpar13 filtrates have a WAT of 24–25 °C; that is, the initial wax concentration does not affect the WAT of the filtrate provided the precipitation and filtration steps occur at the same

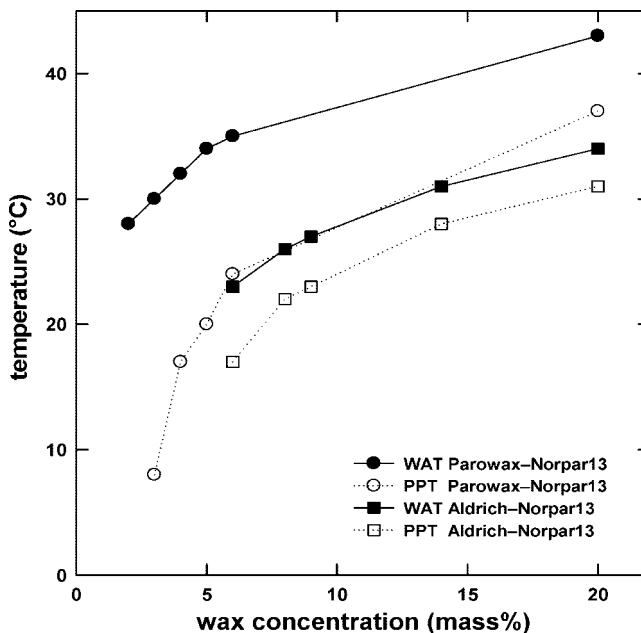


Figure 2. Comparison of WAT and PPT values for Aldrich–Norpar13 and Parowax–Norpar13 mixtures.

(26) Tiwary, D.; Mehrotra, A. K. Phase Transformation and Rheological Behaviour of Highly Paraffinic Waxy Mixtures. *Can. J. Chem. Eng.* **2004**, *82*, 162.



**Table 2. WAT and WDT Values for Filtrates**

Aldrich wax (average room temperature = 24.6 °C)			Parowax (average room temperature = 25.3 °C)		
wax concentration in original wax-solvent mixture (mass %)	WAT (°C)	WDT (°C)	wax concentration in original wax-solvent mixture (mass %)	WAT (°C)	WDT (°C)
8	23	28	2	24	29
9	24	28	3	24	28
			5	24	29
			6	25	28

temperature. Likewise, all Aldrich–Norpar13 filtrates have a WAT of 23–24 °C. It is interesting to note that the WDT of all filtrates is 28–29 °C, which is about 4–5 °C higher than their WAT.

In the previous study,<sup>25</sup> the interface temperature was reported to be about 1 °C lower than the mixture temperature during deposition under static-cooling at temperatures lower than the WAT, such that the mixture consisted of solid and liquid phases. The measured interface temperature was assumed to be equal to the WAT of the liquid phase of the wax–solvent mixture. The results obtained from these precipitation-filtration tests validate this assumption. The results also show that the WAT and WDT of the liquid phase do not vary with the wax concentration in the original wax–solvent mixture.

**Batch Deposition Apparatus.** In the previous study,<sup>25</sup> 14 and 20 mass % Aldrich–Norpar13 mixtures were used in batch deposition experiments under static cooling to determine the liquid–deposit interface temperature. To compare with the results of that study, a 20 mass % Parowax–Norpar13 mixture was used in static cooling experiments. The static cooling apparatus with cooling from the wall<sup>25</sup> was used in these deposition experiments, in which the deposit-layer started at the vessel wall and its growth was radially inward, causing the liquid–deposit interface area to decrease with time.

For deposition experiments with sheared cooling, the static cooling apparatus was modified to include an agitator. The agitator was a plexiglass cylinder, 2.54 cm (or 1 in.) in diameter and 8.9 cm (or 3.5 in.) long, located at the center of the vessel and driven by a motor. Figure 3 shows a schematic of the apparatus with the deposition vessel placed in a temperature-regulated coolant bath. As with the static cooling apparatus, a circular disk of styrofoam insulation, 3.8 cm (1.5 in.) in thickness, was placed at the bottom of the vessel. Another styrofoam disk, 5.1 cm (2 in.) in thickness and 17.8 cm (7 in.) outer radius, was attached at the bottom around the outside of the vessel. The temperatures inside the cylindrical vessel at different radial locations were measured with 7 precalibrated J-type thermocouples. Table 3 lists the thermocouple locations for the static- and sheared-cooling deposition experiments. The thermocouples are labeled TC1 to TC7 based on their distances from the cooling surface. All thermocouples were connected to a data-logger for continuous recording of all temperatures with time on a PC.

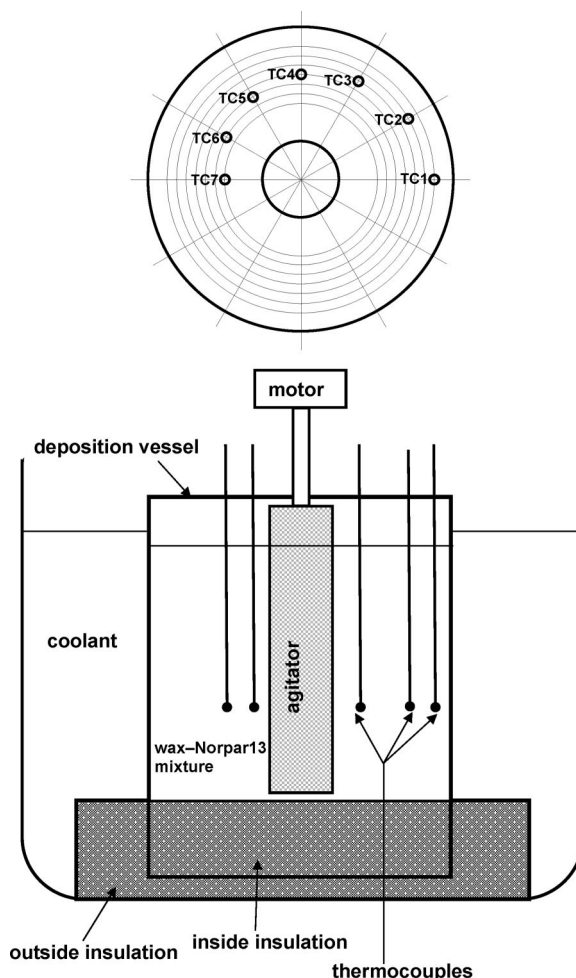
**Deposition Experiments.** All prepared wax–Norpar13 mixtures were heated to 70 °C in a water-bath and held isothermally for 30 min for erasing any thermal history. The wax–Norpar13 mixture was allowed to cool slowly to the initial temperature of WAT + 21 °C, after which it was poured into the deposition vessel.

For the static-cooling experiment with 20 mass % Parowax–Norpar13 mixture, the deposition vessel was placed into the cooling water-bath held at a temperature of WAT – 10 °C. The plexiglass lid with thermocouples was instantly placed on top of the vessel, and the temperature recording was commenced. The experiment was continued until the lowest temperature in the vessel approached the coolant temperature. The static-cooling experiment lasted about 400 min.

For the sheared-cooling experiments, the deposition vessel was placed in the cooling water-bath maintained at the preset coolant temperature, and the agitator was set to the required speed. The 20 mass % Aldrich–Norpar13 mixture, cooled to an initial temperature of WAT + 21 °C, was poured into the vessel. Then, the plexiglass lid with attached thermocouples was instantly placed on top of the vessel, and the temperature recording was commenced. The sheared-cooling experiments were carried out at two agitator speeds of 150

and 300 rpm and with three coolant temperatures of WAT – 5 °C, WAT – 10 °C, and WAT – 20 °C. The deposition experiments were continued until all temperatures in the vessel approached the coolant temperature.

**Couette–Taylor Flow and Shear Rates.** The apparatus for deposition with sheared cooling as described above is similar in principle to the Couette–Taylor configuration, which involves the shearing of a fluid held between two concentric cylinders. Zougari

**Figure 3.** Experimental apparatus for deposition at the vessel wall with sheared-cooling.**Table 3. Radial Distance of Thermocouples from the Wall of Deposition Vessel**

deposition with static cooling		deposition with sheared cooling	
thermocouple number	radial distance from the cooling surface (in.)	thermocouple number	radial distance from the cooling surface (in.)
TC1	0.250	TC1	0.250
TC2	0.375	TC2	0.375
TC3	0.500	TC3	0.500
TC4	0.625	TC4	0.625
TC5	0.750	TC5	0.750
TC6	1.500	TC6	0.875
TC7	2.000	TC7	1.000

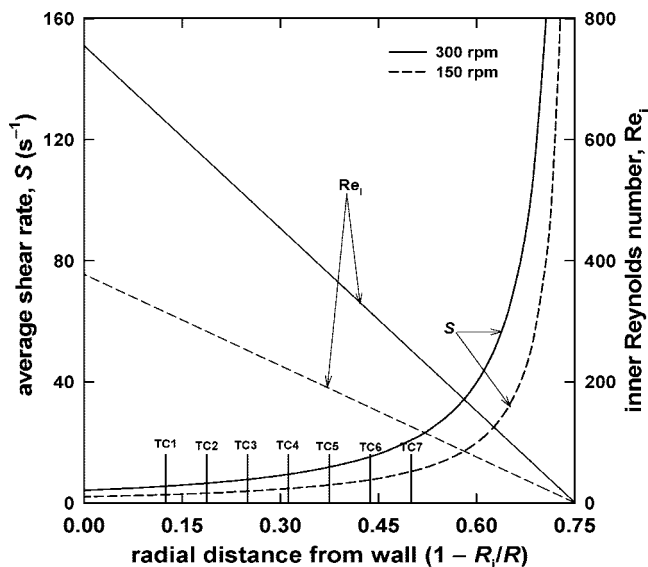


**Figure 4.** Predicted change in average shear rate and inner Reynolds number with radial location during sheared-cooling deposition experiments.

et al. described a deposition apparatus based on the Couette–Taylor flow principles.<sup>27</sup> With the inner cylinder rotating and the outer cylinder held stationary, the inner Reynolds number for the Couette–Taylor flow is given by eq 1,

$$Re_i = \frac{\omega \rho r_i (R_i - r_i)}{\mu} \quad (1)$$

where  $\omega$  denotes the rotational speed, and  $(R_i - r_i)$  is the annular gap between the interface and the inner cylinder (i.e., the agitator). The density ( $\rho$ ) and viscosity ( $\mu$ ) values were obtained from the correlations reported by Fong and Mehrotra.<sup>13</sup> The average shear rate for the Couette–Taylor flow is given by the following relationship:<sup>28</sup>

$$S = \frac{4\pi\omega r_i^2}{(R_i^2 - r_i^2)} \quad (2)$$

For the rotational speeds of 150 and 300 rpm used in the sheared-cooling experiments, the inner Reynolds numbers initially at  $R_i = R$  were 378 and 755, respectively. Figure 4 presents the changes in calculated  $S$  and  $Re_i$  with the radial location. Note that the vertical lines labeled TC1–TC7 indicate the thermocouple locations in the deposition vessel. In Figure 4, the shear rate for a constant agitator speed is predicted to slowly with  $R_i$  initially, but it increases faster as  $R_i \rightarrow r_i$ . On the other hand,  $Re_i$  decreases linearly with an increase in  $R_i$ , that is,  $Re_i \rightarrow 0$  as  $R_i \rightarrow r_i$ .

## Results and Discussion

**Deposition Temperature Profiles.** The radial temperature profile for each thermocouple location in the deposition experiments are discussed in this section. Note that, in all cases, the thermocouple TC1 was the closest to the cooling wall and TC7 the farthest. Also, all thermocouple locations were the same as in the previous study,<sup>25</sup> except TC6 and TC7 which in the sheared-cooling experiments were located away from the center of the vessel due to the centrally placed agitator. Cooling of

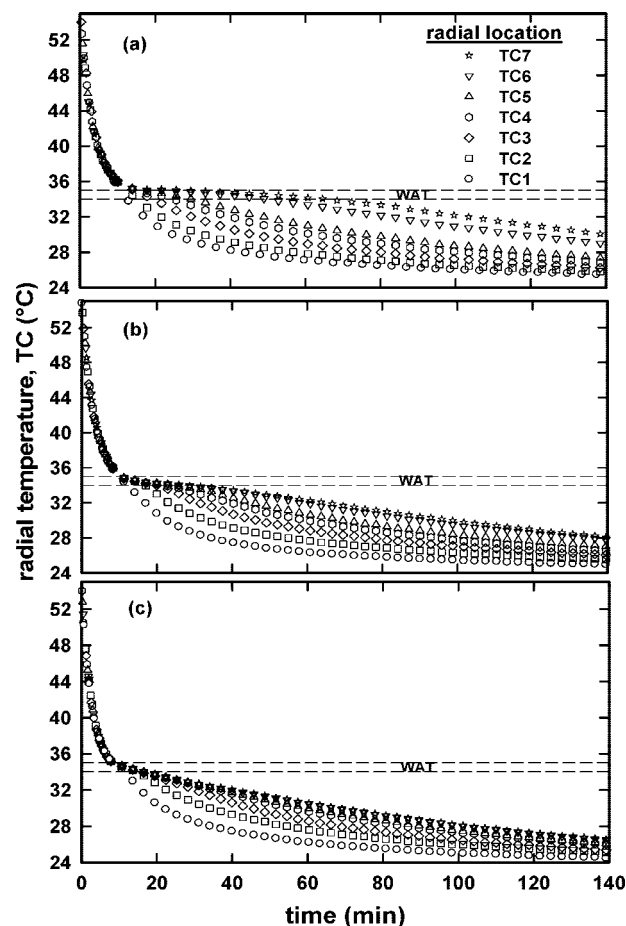


**Figure 5.** Radial temperature profiles during deposition with 20 mass % Aldrich–Norpar13 mixture at coolant temperature of WAT – 10 = 24 °C using; (a) 0,<sup>25</sup> (b) 150, and (c) 300 rpm.

the wax–solvent mixture started at WAT + 21 °C, and the cooling surface was held at WAT – 10 °C in all experiments described in this section.

**Effect of Shear Rate.** Figure 5 presents the temperature profiles obtained during deposition from the 20 mass % Aldrich–Norpar13 mixture under static- and sheared- cooling. Figure 5a shows the results obtained previously<sup>25</sup> from the static-cooling experiment (i.e., without any induced shear). Figures 5b and 5c show the results obtained from sheared-cooling experiments at 150 and 300 rpm, respectively. The region labeled as “WAT” in each case represents the uncertainty in the measured WAT.

It was observed, in all cases, that the temperatures at different radial locations were the same during the initial period of the cooling process. That is, there was no temperature variation in the radial direction until the temperatures approached about 36 °C, after which the temperature at TC1 (closest to the cooling surface) started to decrease faster than those at TC2–TC7. It is pointed out that the temperature at TC1 started changing at a different rate than those at other thermocouple locations due to the liquid–deposit interface reaching the location of TC1, as confirmed by visual observations during deposition under static conditions.<sup>25</sup> The lack of variation in the radial temperatures is attributed to forced convection induced by agitation. For static-cooling experiments, it could be attributed to natural convection and/or liquid circulation induced by volume-shrinkage caused by the cooling and partial solidification of liquid.<sup>25</sup>

After about 50 min of cooling, the results for 0 and 150 rpm shear rates show a radial temperature difference between all the TC1–TC7 temperatures with time, although TC6 and TC7

(27) Zougari, M.; Jacobs, S.; Ratulowski, J.; Hammami, A.; Broze, G.; Flannery, M.; Stankiewicz, A.; Karan, K. Novel Organic Solids Deposition and Control Device for Live-Oils: Design and Applications. *Energy Fuels* **2006**, *20*, 1656.

(28) Dumont, E.; Fayolle, F.; Sobolik, V.; Legrand, J. Wall Shear Rate in the Taylor–Couette–Poiseuille Flow at low Axial Reynolds Number. *Int. J. Heat Mass Transfer* **2002**, *45*, 679.

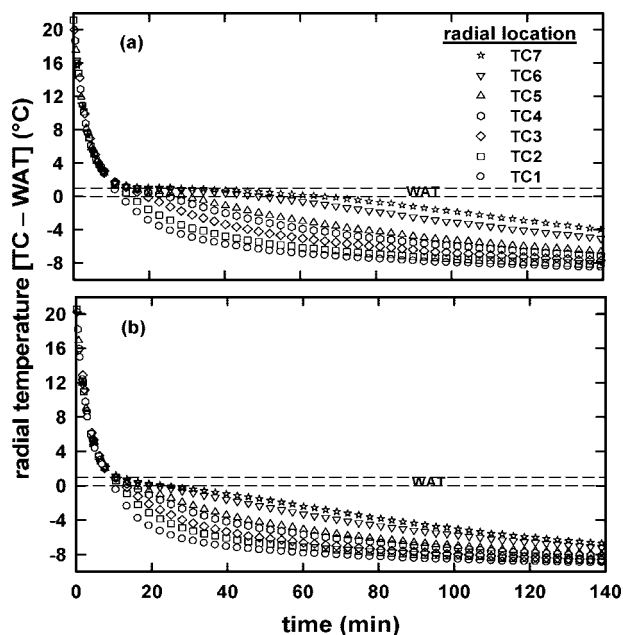


**Figure 6.** Radial temperature profile during deposition under static-cooling at coolant temperature of  $(WAT - 10)^{\circ}C$  (0 rpm); (a) 20 mass % Aldrich-Norpar13<sup>25</sup> and (b) 20 mass % Parowax-Norpar13.

temperatures are almost equal for the 150 rpm experiment. Figure 5c shows that the temperatures at locations TC4–TC7 are also almost equal over the duration of the experiment due to the higher shear rate at 300 rpm. The effect of shear rate on the rate of cooling is distinctively observed at 140 min. At this point, the radial temperature ranges are about 25–30  $^{\circ}C$  for no shear, 25–28  $^{\circ}C$  for 150 rpm, and 24–26  $^{\circ}C$  for 300 rpm. Thus, at a higher shear rate, the cooling is faster with a smaller radial temperature variation.

**Results with Different Waxes.** Figure 6 compares similar temperature profiles obtained with 20 mass % Aldrich-Norpar13 and Parowax-Norpar13 mixtures under static cooling. Because these two mixtures have different WAT values, the radial temperatures have been presented as the difference between the thermocouple temperature and the WAT of each mixture. For both sets of results, it is again observed that there was no temperature variation in the radial direction initially (i.e., until the liquid–deposit interface reaches close to TC1 and a temperature of about  $TC - WAT = 1\text{--}2^{\circ}C$ ). Afterward, the Parowax-Norpar13 mixture in Figure 6b is cooled faster and has a narrower radial temperature variation, compared to the Aldrich-Norpar13 mixture in Figure 6a.<sup>25</sup> For example, at 140 min, the Aldrich-Norpar13 mixture shows  $TC7 - WAT = -4^{\circ}C$ , whereas the Parowax-Norpar13 mixture has cooled to a lower value of  $-7^{\circ}C$ . Moreover,  $TC7 - TC1 = 4.5^{\circ}C$  for the Aldrich-Norpar13 mixture, whereas  $TC7 - TC1 = 2^{\circ}C$  for the Parowax-Norpar13 mixture.

**Temperature Variation at TC7.** Figure 7a presents the temperature variation at the thermocouple location TC7 for deposition experiments carried out with 20 mass % Aldrich-Norpar13 mixtures under static and sheared cooling, and Figure 7b compares similar results with both waxes under static cooling. The change in temperature during the initial cooling period is the same for all wax–solvent mixtures, which is not affected by the shear rate or the wax type. The temperatures for different shear rates and wax type start to deviate when each mixture reaches its WAT. Cooling of the 20 mass % Aldrich-Norpar13 mixture at 300 rpm occurred at the fastest pace in sheared-cooling experiments, whereas the 20 mass % Parowax-Norpar13 mixture cooled faster in static-cooling experiments.

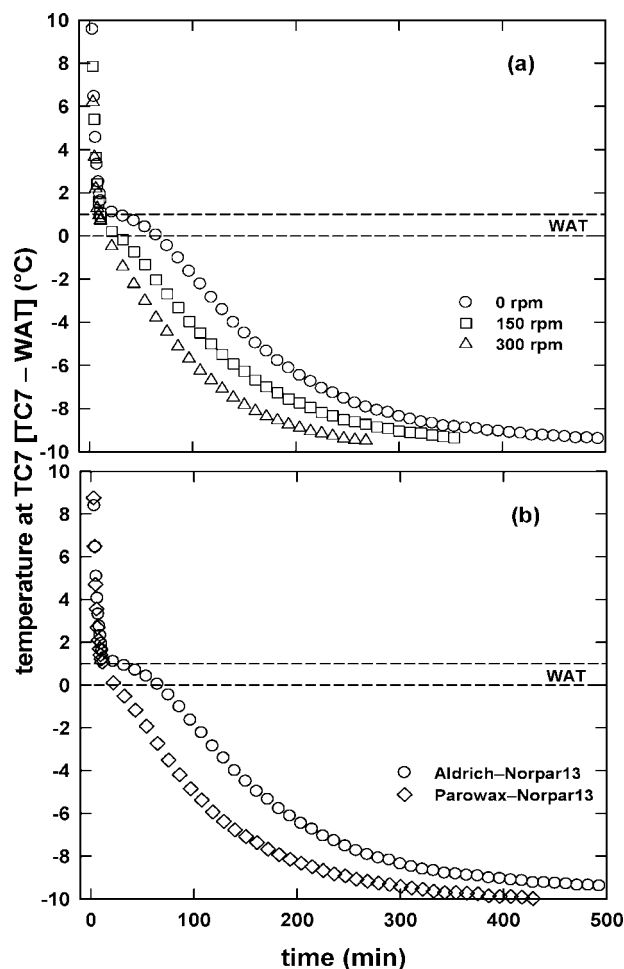


**Figure 7.** Temperature profile of thermocouple TC7 at coolant temperature of  $(WAT - 10)^{\circ}C$ ; (a) 20 mass % Aldrich-Norpar13 mixture under sheared-cooling and (b) 20 mass % Aldrich-Norpar13 and Parowax-Norpar13 mixtures under static-cooling.

As shown in Table 3, thermocouple TC7 was farthest from the cooling surface. For the two static-cooling experiments (with TC7 at the center of the vessel) with 20 mass % Parowax-Norpar13 and Aldrich-Norpar13 mixtures, it was observed that the deposit had advanced to the location of TC7 at the end of the experiment. However, for the two sheared-cooling experiments (with TC7 not at the center and away from the agitator surface) with 20 mass % Aldrich-Norpar13 mixture, the deposit-layer did not advance to the location of TC7 even after the entire vessel content had reached the coolant temperature. That is, for the sheared-cooling experiments, a liquid region continued to exist between the deposit and the agitator surface.

**Liquid–Deposit Interface Location.** The temperature at each of the seven thermocouple locations was monitored with time until all of the temperatures, TC1 to TC7, became close to the coolant temperature. Visual monitoring of the growth of the liquid–deposit interface was difficult for both sheared- and static-cooling experiments because the liquid-region temperature reached the WAT well before the interface reached halfway radially across the vessel, at which point the liquid region became cloudy. The interface location was, therefore, obtained by analyzing the rate of change of temperature,  $dT/dt$ , at each thermocouple location.<sup>25</sup> This method is illustrated in Figure 8, where  $dT/dt$  values are plotted against time for the sheared-cooling experiment at 300 rpm with a coolant temperature of  $WAT - 5 = 29^{\circ}C$ . The average time and temperature of the highlighted regions correspond to the location of the interface



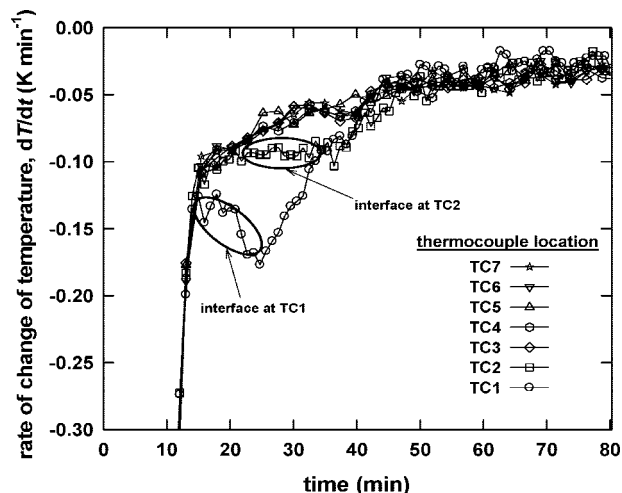


**Figure 8.** Determining the interface location from the rate of change of temperature for 20 mass % Aldrich-Norpar13 mixture at coolant temperature of WAT - 5 = 29 °C and 300 rpm.

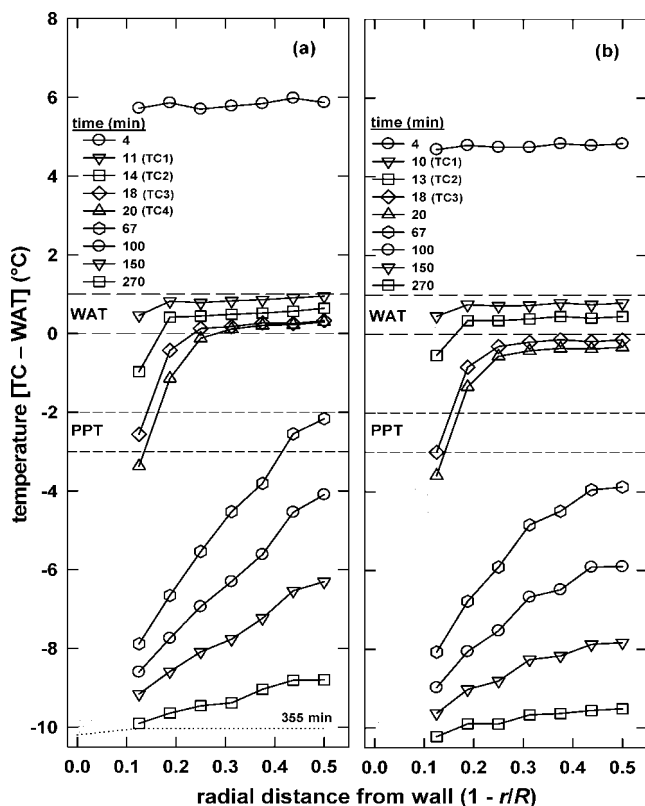


**Figure 9.** Changes in radial temperature profile with time during deposition under sheared-cooling of 20 mass % Aldrich-Norpar13 mixture at coolant temperature of WAT - 10 = 24 °C; (a) 150 rpm and (b) 300 rpm.

at the radial locations of TC1 and TC2. As shown in Figure 8, the curves for TC3–TC7 do not show a similar plateau. Thus, the region beyond TC2 contained liquid even after the mixture temperature had decreased to the coolant temperature.

The  $dT/dt$  method was used for each set of temperature versus time data from all deposition experiments, and the results are presented in the following sections. Note that this method was used to estimate the interface location corresponding to thermocouples TC1–TC4.<sup>25</sup>

**Changes in Radial Temperature Profile with Time.** Figure 9 shows the radial temperature profiles with time for deposition experiments with 20 mass % Aldrich-Norpar13 mixture at a coolant temperature of WAT - 10 °C (or 24 °C) at 150 and

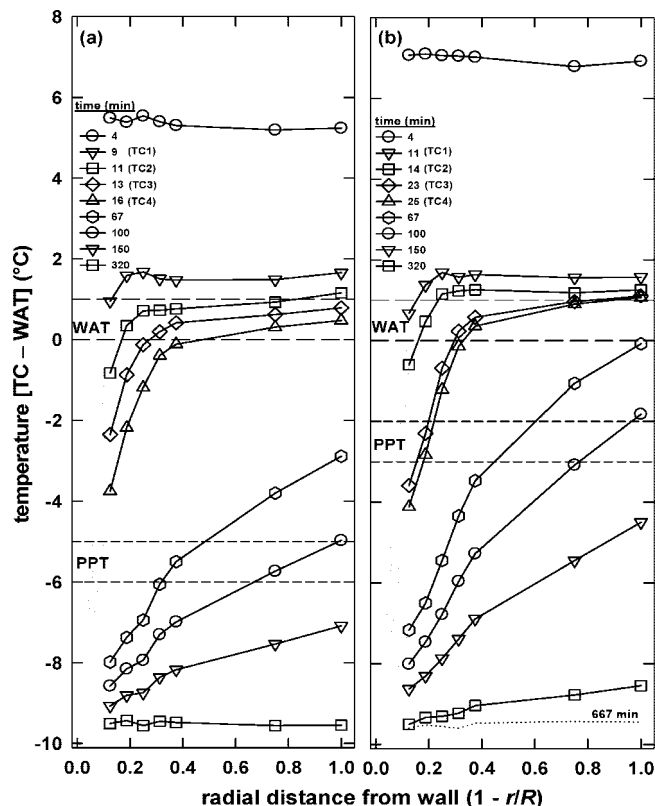


**Figure 10.** Changes in radial temperature profile with time during deposition under static-cooling at coolant temperature of (WAT - 10)°C; (a) 20 mass % Parowax-Norpar13 mixture and (b) 20 mass % Aldrich-Norpar13 mixture.

300 rpm. In each plot, the times labeled TC1–TC4 indicate the time for the liquid–deposit interface to reach those locations. A comparison of the radial temperature profiles in the two plots of Figure 9 shows that cooling occurred faster at higher rpm. The higher agitation speed also initially caused a faster interface movement. The temperatures at 300 rpm approached the coolant temperature about 85 min earlier than those at 150 rpm. At the conclusion of the experiment at 300 rpm, even though the temperature throughout the vessel was close to the coolant temperature and well below the PPT of the original Aldrich-Norpar13 mixture, the liquid–deposit interface had not reached TC4. Under similar conditions for the experiment at 150 rpm, the interface did not advance past thermocouple TC5.

Figure 10 compares the variation of radial temperature profiles with time for the static-cooling experiment with 20 mass % Parowax-Norpar13 mixture and those reported previously for 20 mass % Aldrich-Norpar13 mixture.<sup>25</sup> The coolant temperature in both cases was WAT - 10 °C. At  $t = 4$  min, the temperature in the liquid region was the same at all radial locations for both mixtures; however, the Parowax-Norpar13 mixture had cooled to a lower temperature. As shown in Figures 10a and 10b, the interface reached TC1 at  $t = 9$  and 11 min, respectively, whereas the liquid region remained above the respective WAT. At  $t = 11$  and 14 min, the interface reached TC2 for the two cases, respectively. The interface movement afterward slowed down considerably. In Figure 10b, for the Aldrich-Norpar13 mixture, the interface reached TC3 at  $t = 23$  min, and it reached TC3 at  $t = 13$  min for the Parowax-Norpar13 mixture in Figure 10a. At these same cooling times, the liquid region temperature reached the respective WAT for both mixtures. The interface reached TC4 at  $t = 16$  and 25 min in Figures 10a and 10b, respectively. Although the PPT of the Parowax-Norpar13 mixture is 3 °C lower than that of the

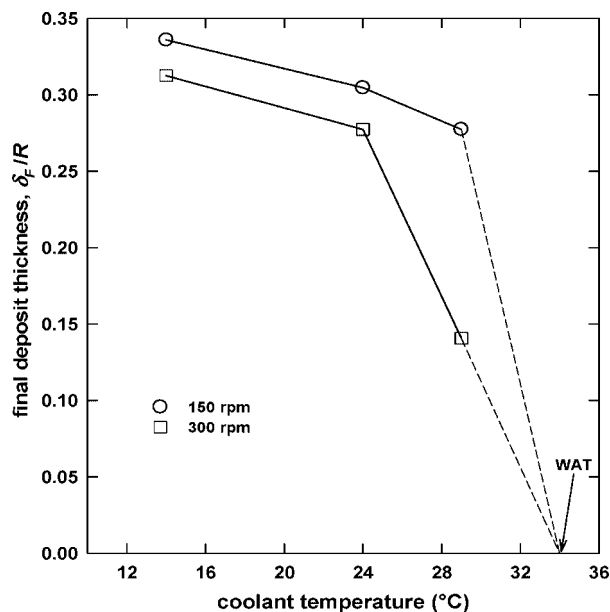


**Figure 11.** Final deposit thickness obtained during sheared-cooling at 150 and 300 rpm of 20 mass % Aldrich–Norpar13 mixtures at varying coolant temperatures.

Aldrich–Norpar13 mixture, TC7 reached the PPT at about the same time of  $t = 100$  min for both mixtures due to the faster cooling of the Parowax–Norpar13 mixture. At  $t = 320$  min, the temperature of the Parowax–Norpar13 mixture reached within 0.5 °C of the coolant temperature; however, for the Aldrich–Norpar13 mixture, it took about 347 min longer (at  $t = 667$  min). These results showed that the static cooling occurred faster for the Parowax–Norpar13 mixture, which has a lower PPT.

**Effect of Shear Rate on Final Deposit Thickness.** In the previous section, it was observed that, in sheared-cooling experiments at coolant temperatures below the PPT, the deposit grew until it reached a final thickness that varied with the agitator speed (or the induced shear stress). For example, the interface for 20 mass % Aldrich–Norpar13 mixture experiments at 300 rpm did not advance to TC4 except when the coolant temperature was  $\text{WAT} - 20 = 14$  °C. That is, TC4–TC7 continued to be in the liquid region even after the agitation was stopped for several hours. On the other hand, for static-cooling experiments under similar conditions, the deposit continued to grow until it occupied the entire deposition vessel.

At the end of each sheared-cooling experiment (after the temperature throughout the vessel approached the coolant temperature), the final deposit thickness ( $\delta_F$ ) was measured. These final deposit thickness results, expressed as  $\delta_F/R$ , for the two agitator speeds are presented in Figure 11. The trends in Figure 11 indicate that the final deposit thickness ( $\delta_F/R$ ) increased with a decrease in both the coolant temperature and the agitator speed. At the highest coolant temperature of 29 °C, the interface was observed to grow only up to the TC2 location for 300 rpm and to the TC3 location for 150 rpm. The deposit at this coolant temperature was observed to be softer, which is attributed to a lower thermal driving force. Note that, as indicated by dashed-lines in Figure 11,  $\delta_F/R = 0$  when the coolant temperature is equal to the WAT, at which point no deposition would occur due to a lack of thermal driving force.

The continued presence of a liquid phase in the annular region between the final liquid–deposit interface (corresponding to the final deposit thickness) and the agitator surface, at a temperature well below the WAT of the original wax–solvent mixture, suggests that its WAT was at or below the coolant temperature.

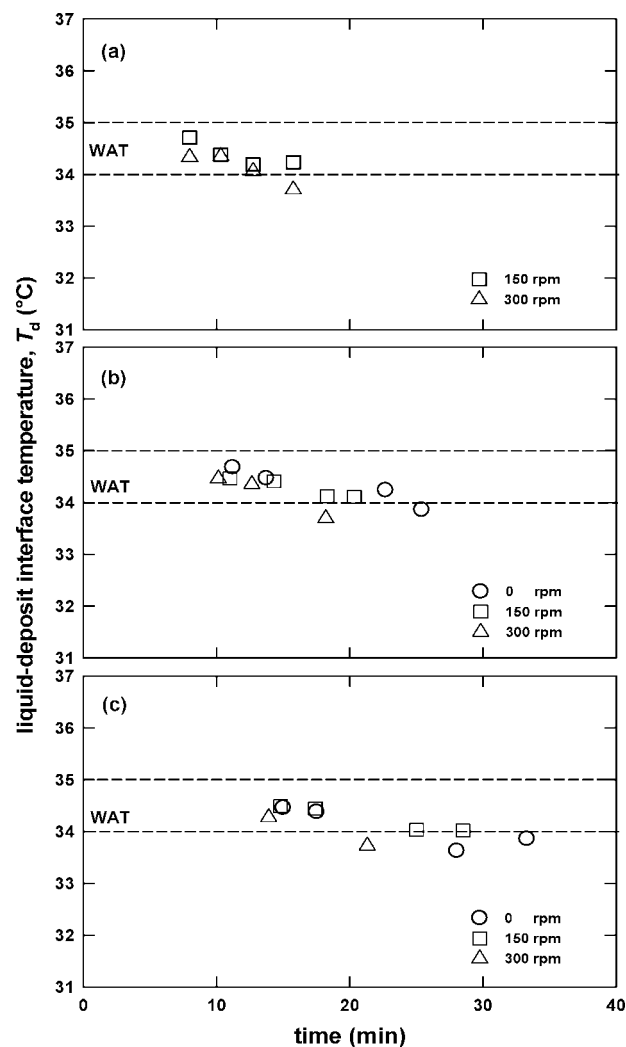


**Figure 12.** Variation in interface temperature ( $T_d$ ) with time for 20 mass % Aldrich–Norpar13 mixture at different shear rates and coolant temperatures; (a)  $\text{WAT} - 20 = 14$  °C, (b)  $\text{WAT} - 10 = 24$  °C, and (c)  $\text{WAT} - 5 = 29$  °C.

A lowering of its WAT could be due to a combination of its decreased wax content and/or heavier *n*-alkane concentrations relative to the original wax–solvent mixture. For these batch experiments, this would imply that the deposit became enriched in wax and/or heavier *n*-alkanes. It is pointed out that a similar enrichment of deposit-layer has also been reported from deposition experiments under both laminar and turbulent flows.<sup>11–13,19</sup>

**Liquid–Deposit Interface Temperature,  $T_d$ .** The  $dT/dt$  method also allowed the estimation of the time taken for the interface to reach each of TC1 to TC4 locations, corresponding to the interface temperature,  $T_d$ .<sup>25</sup> The interface temperature results for the sheared-cooling of 20 mass % Aldrich–Norpar13 mixture are presented in Figure 12 for three coolant temperatures of  $\text{WAT} - 20$  °C = 14 °C,  $\text{WAT} - 10$  °C = 24 °C, and  $\text{WAT} - 5$  °C = 29 °C. Also included in Figures 12b and 12c are similar results from static-cooling experiments, that is, at 0 rpm.<sup>25</sup> For all coolant temperatures, the  $T_d$  values at earlier times are within the WAT region. In Figure 12a, for the lowest coolant temperature of  $\text{WAT} - 20 = 14$  °C, the time taken for the interface to reach radial locations corresponding to TC1–TC4 is not affected by the agitator speed. In Figures 12b and 12c, the interface movement became faster at 300 rpm at coolant temperatures of  $\text{WAT} - 10 = 24$  °C and  $\text{WAT} - 5 = 29$  °C, respectively.

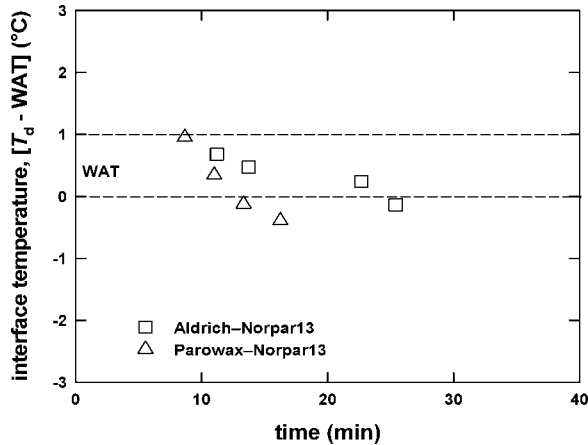


**Figure 13.** Variation in  $T_d$  with time for static-cooling of Aldrich-Norpar13 and Parowax-Norpar13 mixtures at coolant temperature of WAT - 10 °C.

The results in Figure 12 indicate that the interface movement slowed down after reaching the thermocouple location TC2. This slowing down of the interface movement is attributed to the increased thermal resistance offered by the deposit and the liquid being cooled to the WAT, which caused the release of latent heat by wax crystals suspended in the liquid region. For the sheared-cooling experiments, the increased deposit thickness also caused a decrease in  $(R_i - r_i)$ , thereby decreasing  $Re_i$  and increasing  $S$  according to eqs 1 and 2.

The  $T_d$  values at longer times in Figure 12 are lower and slightly below the WAT. The temperature measurements for these cases showed the liquid region temperature to be close to or below the WAT. It was observed that, when the liquid temperature reached the WAT, it became a two-phase mixture with (solid) crystals suspended in the liquid phase. As shown by the precipitation-filtration tests, the lower  $T_d$  values in these cases would be equal to the WAT of the liquid phase (whose wax content was lowered due to the formation of wax crystals). Hence, all  $T_d$  results from sheared- and static-cooling experiments can be considered to be equal to the WAT of the liquid phase.

Figure 13 compares the results for  $T_d$  obtained from static-cooling experiments with 20 mass % Parowax-Norpar13 and Aldrich-Norpar13 mixtures at the coolant temperature of WAT - 10 °C. Again, both sets of  $T_d$  results are within or slightly below the WAT region. The interface was observed to move faster for the Parowax-Norpar13 mixture than the Aldrich-Norpar13 mixture, which, as mentioned before, is due to the faster cooling of the Parowax-Norpar13 mixture. Differences between the carbon number distributions for the two waxes could explain the observed differences in the movement of the interface. It is also pointed out that (WAT - PPT) for the 20 mass % Parowax-Norpar13 mixture is 6 °C, whereas it is 3 °C for the 20 mass % Aldrich-Norpar13 mixture. Overall, the results in Figures 12 and 13 for the mixtures prepared with two different waxes and tested under static- and sheared-cooling indicate that the liquid-deposit interface temperature ( $T_d$ ) is essentially equal to the WAT of the liquid phase. This observation supports the constant-interface-temperature assumption in the heat-transfer approach for solids deposition.<sup>11-13,19-21,25</sup>

#### Deposit-Layer Thickness (or Interface Radial Location).

Figures 14 and 15 present the interface temperature results included in Figures 12 and 13 as a function of the deposit thickness,  $\delta/R$  (or the radial location of the interface). In Figure 14, the  $T_d$  values for Aldrich-Norpar13 mixtures at all radial locations are not appreciably affected by the agitator speed (or

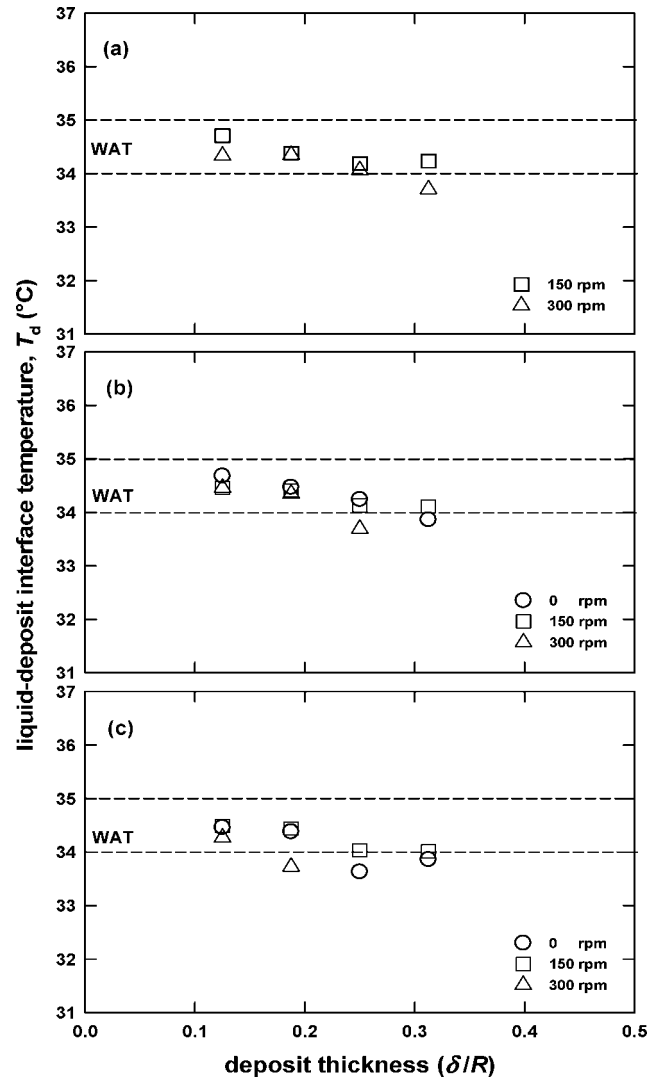


**Figure 14.** Variation in  $T_d$  with radial location for sheared-cooling of 20 mass % Aldrich-Norpar13 mixture at different shear rates and coolant temperatures; (a) WAT - 20 = 14 °C, (b) WAT - 10 = 24 °C, and (c) WAT - 5 = 29 °C.

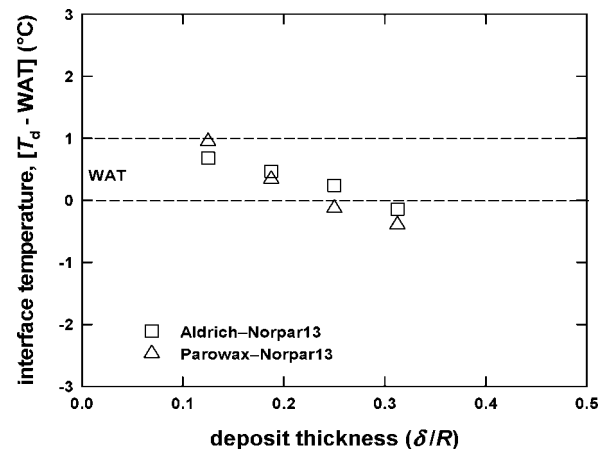


**Figure 15.** Variation in  $T_d$  with radial location for static-cooling of Aldrich-Norpar13 and Parowax-Norpar13 mixtures at a coolant temperature of WAT - 10 °C.

shear rate). Also, the  $T_d$  values are not influenced by the coolant temperature. The results from static-cooling experiments with different waxes, plotted in Figure 15, show that the  $T_d$  values are essentially the same at each radial location. However, the  $T_d$  values decrease somewhat with the growth of the deposit,

which, as previously mentioned, is attributed to the lowering of the liquid-phase WAT caused by the precipitation of wax particles.

In summary, the results in Figures 12–15 show that the liquid–deposit interface temperature ( $T_d$ ) remains constant at WAT when the liquid-region temperature is higher than or equal to the WAT of the original wax–solvent mixture. Once the liquid-region temperature becomes less than the WAT,  $T_d$  decreases slightly to the “effective” WAT of the liquid phase, as confirmed by the precipitation-filtration experiments. That is, the liquid–deposit interface temperature ( $T_d$ ) at all times is equal to the WAT of the liquid phase. This observation is supportive of the constant-interface-temperature assumption in the heat-transfer approach for modeling solids deposition; that is, the liquid–deposit interface temperature during the formation and growth of deposit layer from “waxy” mixtures is equal to the WAT of the liquid phase. Thus, the results of this study provide a framework for estimating the temperature profile during deposition from waxy crude oils flowing in a pipeline. Furthermore, this study offers additional confirmation that the wax deposition process is governed primarily by the rate of heat transfer.

### Conclusions

A series of experiments were carried out to study the formation and growth of deposit-layer during the cooling of wax–solvent mixtures under sheared- and static-cooling. The results from these experiments allowed the determination of the liquid–deposit interface temperature at different radial locations with time under sheared- and static-cooling conditions performed with a range of coolant temperatures.

Precipitation-filtration experiments were described for determining the WAT of the liquid portion of a wax–solvent mixture, when held at a temperature below the WAT. These tests showed that the WAT of filtrate was 1–2 °C below the filtration and precipitation temperature. The initial wax concentration in the wax–solvent mixture did not affect the WAT and WDT of the filtrate.

Deposition experiments were performed under sheared- and static-cooling conditions. The static-cooling experiments with Parowax–Norpar13 mixtures confirmed the observations previously reported with another wax sample.<sup>25</sup> In sheared-cooling experiments, the deposit achieved a final thickness that depended on the agitator speed (or the shear rate). In all experiments, the liquid–deposit interface temperature during the initial growth of deposit-layer remained equal to the WAT of the wax–Norpar13 mixture, and it slightly decreased as the liquid region temper-

ature became less than the WAT. Below the WAT, the liquid region became a “cloudy” two-phase mixture with crystals suspended in the liquid phase, and the decrease in the interface temperature was attributed to the lowering of the WAT of the liquid phase.

Overall, the results from deposition experiments carried out at different shear rates, compositions, and coolant temperatures indicated that the liquid–deposit interface temperature ( $T_d$ ) under both sheared- and static-cooling was equal to the WAT of the liquid phase. That is, the results did not show the interface temperature to increase from an initial value close to the wall (or coolant) temperature to reach the WAT ultimately, which is an important assumption in the molecular diffusion approach for modeling wax deposition. On the other hand, the results of this study, together with those recently reported,<sup>25</sup> provided a validation of the constant-interface-temperature assumption made in the heat-transfer approach for modeling solids deposition from waxy mixtures. This indicated that the wax deposition process during the transportation of waxy crude oils in pipelines is primarily governed by the rate of heat transfer.

**Acknowledgment.** Financial support was provided by the Natural Sciences and Engineering Research Council of Canada (NSERC) and the Department of Chemical and Petroleum Engineering, University of Calgary. We thank Mr. Bernie Then and Ms. Elizabeth Zalewski for their technical and analytical support.

### Nomenclature

$r$  = radial distance (m)  
 $r_i$  = (outside) radius of agitator rod (m)  
 $R$  = (inside) radius of cylindrical vessel (m)  
 $R_i$  = radial location of liquid–deposit interface (m)  
 $Re_i$  = inner Reynolds number for Couette–Taylor flow  
 $S$  = average shear rate ( $s^{-1}$ )  
 $t$  = time (min)  
 $T$  = temperature (°C)  
 $T_d$  = liquid–deposit interface temperature (°C)

### Greek Letters

$\delta$  = deposit thickness [=  $R - R_i$ ] (m)  
 $\delta_F$  = final deposit thickness (m)  
 $\mu$  = viscosity of wax–solvent mixture (Pa s)  
 $\rho$  = density of wax–solvent mixture ( $kg\ m^{-3}$ )  
 $\omega$  = rotational speed ( $rev\ s^{-1}$ )

### Acronyms

PPT = pour point temperature (°C)  
WAT = wax appearance temperature (°C)  
WDT = wax disappearance temperature (°C)

EF800542A